ing for the cutoff frequencies of 900MHz, 1.0 and 1.1GHz by setting I_{O2} to 40, 52 and 66μA, respectively. It can be seen that a zero (defined by eqn. 2) placed very close to 2GHz shifts the roll-off characteristics away from –80dB/dec. This effect can be alleviated by increasing the transconductances of M1 and M2 to push the zero to higher frequencies. However, this can be accomplished at the expense of power consumption. Table 1 indicates spurious-free dynamic range (SFDR), 1%-THD dynamic range (DR) and power dissipation (P_{diss}) of the filter at different cutoff frequencies (f_O).

Conclusions: A low-power very-high-frequency current-mode filter based on vertical stacking of regulated cascode biquads has been realised. Around a GHz region, moderate dynamic range can be obtained under low-power consumption owing to bias current sharing and simple topology.

 2 January 2001

Electronics Letters Online No: 20010251
DOI: 10.1049/el:20010251

U. Yodprasit and K. Sirivathanant (*Mahanakorn University of Technology, Cheum-Sampan Road, Bangkok 10530, Thailand*)

E-mail: uroschanit@mail.ee.mut.ac.th

References

1 NGARMNIL, J., and TOUMAZOU, C.: 'New approach for high order-high frequency analogue micropower filter design'. IEEE Int. Symp. Circuits and Systems, June 1997, Vol. 1, pp. 85–88

3D tetrahedron ray tracing algorithm

Z. Zhang, Z. Yun and M.F. Iskander

A new three-dimensional (3D) tetrahedron meshed ray tracing (TMRT) method is proposed. It is based on dividing the propagation region into tetrahedral cells whereby the number of tetrahedrons is decided by the number of vertices of structures instead of their dimensions. This method represents a 3D extension to the 2D procedure described in an earlier paper. Results from the 3D TMRT method show significant improvement in computational efficiency and are typically less than one half of those of the visibility ray tracing approach. These results were illustrated by calculating the delay spread in a typical indoor propagation environment.

Introduction: Propagation prediction is very important in the design of wireless communications systems. The ray tracing method has become a vital tool for calculating parameters such as delay spread, angle of arrival, and coverage in typical wireless communication environments. This is especially true for the micro- and pico-cell cases where site-specific propagation information is needed in developing high-quality communication systems [1].

The conventional ray tracing method is based on a ray-launching and bouncing procedure which can be very inefficient if no speed-up algorithm is employed. Several schemes have been developed to accelerate the ray tracing procedure, e.g. the image method, the bounding box method, and the utilisation of visibility [2, 3]. Although these methods have advantages, a more efficient method is needed to cope with the complex and often computationally demanding indoor or indoor/outdoor situations while maintaining good accuracy of the propagation prediction results. An efficient ray tracing method based on triangular division of the propagation space has been studied in the two-dimensional (2D) case [4]. In this Letter we extend the 2D triangular-based algorithm described earlier to a 3D tetrahedron-based algorithm. It is of significant interest to examine the impact of the 3D implementation of the proposed procedure on the computational savings reported earlier for the 2D case.

TMRT method: It is generally known that 3D structures can be discretised by tetrahedrons. These tetrahedrons may be meshed such that they are based on the vertices of the object. This discretisation procedure is somewhat different from normal meshing methods routinely used in numerical methods such as the finite element method, where mesh refinement procedures are often implemented to improve the accuracy of the results. In the proposed method, discretisation is related to only the existing vertices of the object and no auxiliary ones are introduced. In the TMRT method, the size of the tetrahedrons has no effect on accuracy, but the number of tetrahedrons clearly plays a role in determining the efficiency of the proposed algorithm. Hence we implemented a digitisation procedure that is related only to the vertices of the object in the propagation environment.

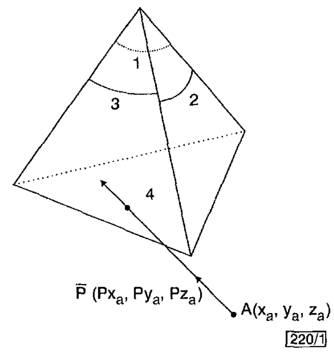

Fig. 1 *Intersection test on tetrahedron*

Fig. 1 shows a typical tetrahedral cell which may be encountered in the proposed method. After discretising the propagation domain, the key remaining step in the solution procedure involves the determination of which face of a specific tetrahedron will be hit by the incident ray as it continues to propagate in a communication environment. As may be noted from Fig. 1, there are four faces – faces 1, 2, 3 and 4 – in a tetrahedron. Assuming there is a ray incident into the tetrahedron from point A through face 4, there will be only three faces – faces 1, 2 and 3 – that can possibly be hit by the incident ray. After deciding the hit face, as will be described later, there are two kinds of interactions that can be considered. In one case, the hit face is a real wall and hence the cross point, the reflect, and the transmit rays will need to be calculated. In the other situation, the hit face is an auxiliary face, in which case the ray will continue to propagate directly towards the next neighbouring tetrahedron and the solution procedure will continue as described above. Because all of the information about the adjacent tetrahedron related to each face is known, the ray can quickly go through from one tetrahedron to another by a 'pointer-locating' method instead of requiring time-consuming searching algorithms. Avoiding the use of a search algorithm to determine the 'next' hit surface constitutes the main computational advantage of the proposed method.

Consider the tetrahedral cell shown in Fig. 1. The incident ray is originating from point A (x_a, y_a, z_a) and is propagating with normalised direction vector $\bar{P}(Px_a, Py_a, Pz_a)$. Hence, the line describing the incident ray parameters is defined as

$$\begin{aligned} x &= x_a + Px_a * \Delta l \\ y &= y_a + Py_a * \Delta l \\ z &= z_a + Pz_a * \Delta l \end{aligned} \tag{1}$$

Δl in eqn. 1 is a variable that represents the incremental change in the line length along the ray.

The tetrahedral faces 1, 2, 3 and 4, can be defined by

$$a_i * x + b_i * y + c_i * z + d_i = 0 \qquad (i = 1, 2, 3, 4) \tag{2}$$

Substituting eqn. 1 into eqn. 2, we obtain

$$\Delta l_i = -\frac{a_i * x_a + b_i * y_a + c_i * z_a + d_i}{a_i * Px_a + b_i * Py_a + c_i * Pz_a} \qquad (i = 1, 2, 3, 4) \tag{3}$$

Using eqn. 3 and through the calculation of Δl_i for each tetrahedral face, one can determine the ray hit surface and also the point of intersection. To begin with, when the denominator in eqn. 3 is zero, the ray will be parallel to the plane and there will be no intersection. By the sign of the denominator, inner faces which can be seen from point A along direction $\bar{P}$ can be decided and only those faces need extensive calculation of the length Δl_i, e.g. in the case shown in Fig. 1, only faces 1 and 3 can be seen by the incident ray.

Because tetrahedrons are formed by triangular edges, the face that produces the minimum Δl_i is the hit face. If there are two equally minimum positive Δl_i, the cross edge between two faces which produces the minimum Δl_i, is the one that will be hit by the propagating ray. If there are three equally minimum positive values of Δl_i, the vertex opposite to the incident face is the one that will be hit in this case.

Once again, if the hit face is an auxiliary face, no intersection point calculation is needed; calculations will just proceed to the next tetrahedron and the solution procedure will be repeated. If the hit face is a real wall, the calculated value of Δl_i from eqn. 3 is substituted in eqn. 1 and the coordinates of the intersection point will be obtained.

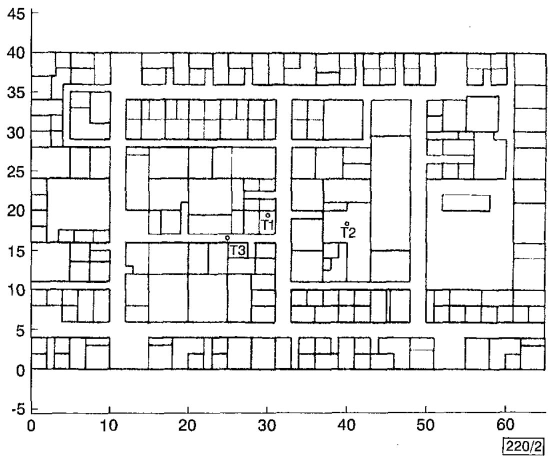

Fig. 2 *Layout and transmitter position*

Table 1: 3D ray tracing results

	TMRT	Vis	Ratio (TMRT/Vis)
	s	s	%
T1	24.2	70.2	34
T2	18.6	46.8	39
T3	21.5	51.6	42
Average	21.4	56.2	38

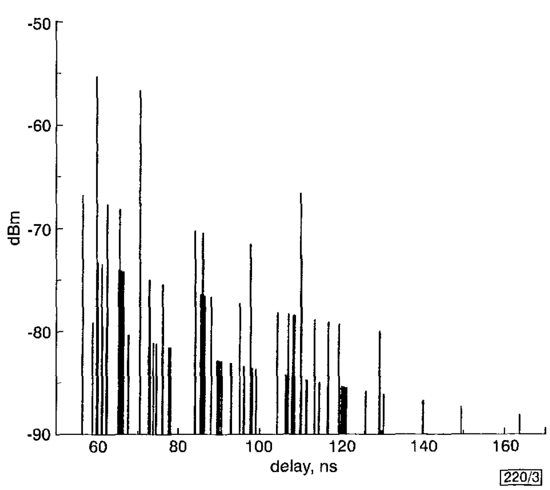

Fig. 3 *Time delay result*

Results: Fig. 2 shows a layout of the third floor of the MEB building at the University of Utah. The volume of this floor is 65 × 40 × 2.5m^3. There are three transmitters: T1 is located in a standard room with only four side walls, T2 is located in a special room with eight side walls, and T3 is located in a hall. Transmitting rays with directions θ ranging from –80° to 80° with step 10° and φ ranging from degree 1° to 360° with step 1° were simulated. Thus, a total of 6120 start rays were included in the calculations. Each ray was allowed to bounce ten times before terminating the calculations. At each bounce, a ray will split to a reflected and a transmitted ray; therefore it is possible that one initial ray can be split to up to 2^{10} rays. If the transmitted ray ends up out of the whole structure, it will be dropped from the calculations.

Table 1 shows the 3D ray tracing results. Simulations were made on a SUN Ultra-80 computer and the compile software is Fortran 90. Comparing the results with those using the visibility method, the average computation time of the proposed tetrahedron method is 38% of the standard visibility approach.

Fig. 3 shows the delay spread results for rays transmitted from T2 and received at T3, assuming that at each bounce the power will be equally split between the transmitted and reflected rays. These delay spread results illustrate the improvement in the computational efficiency. The detailed power distribution pattern (coverage) will be reported in a separate paper.

10 January 2001
Electronics Letters Online No: 20010250
DOI: 10.1049/el:20010250

Z. Zhang, Z. Yun and M.F. Iskander (*Electrical Engineering Department, University of Utah, Salt Lake City, UT 84112, USA*)

References

1 SEIDEL, S.Y., and RAPPAPORT, T.S.: 'Site-specific propagation prediction for wireless in-building personal communication system design', *IEEE Trans. Veh. Technol.*, 1994, **43**, (4), pp. 879–891

2 CATEDRA, M.F., PEREZ DE ADANA, J., and GUTIERREZ, O.: 'Efficient ray-tracing techniques for three-dimensional analyses of propagation in mobile communications: application to picocell and microcell scenarios', *IEEE Antennas Propag. Mag.*, 1998, **40**, (2), pp. 15–28

3 LIANG, G., and BERTONI, H.L.: 'A new approach to 3-D ray tracing for propagation prediction in cities', *IEEE Trans. Antennas Propag.*, 1998, **46**, (6), pp. 853–863

4 ZHANG, Z., YUN, Z., and ISKANDER, M.F.: 'Ray tracing method for propagation models in wireless communication systems', *Electron. Lett.*, 2000, **36**, (5), pp. 464–465

Linearly polarised radial stub fed high performance wideband slot antenna

P.H. Rao, V.F. Fusco and R. Cahill

A wideband printed slot antenna fed by a radial stub operating over the mobile communication bands PCN (1.716–1.880GHz) and UMTS (1.9–2.0GHz and 2.1–2.2GHz) is presented. The impedance bandwidth of the antenna achieved for a *VSWR* ≤ 2 is 34% and the radiation patterns remain stable over the entire frequency band of operation (1.7–2.4GHz) with cross-polarisation levels of less than –20dB. Simulated and measured radiation pattern and return loss results are presented.

Introduction: A major advantage of the slot antenna over dipole antenna configurations is the higher bandwidth that can be achieved and the lower feed interaction effect with respect to radiation pattern influence. To achieve operation over a broad band of frequencies, various methods of feeding the slot antenna have been attempted [1, 2]. In this Letter we show that by using a radial stub as a series element on a 50Ω feeder line we can achieve a wide impedance bandwidth match and stable radiation patterns over the frequency range 1.7–2.4GHz, covering PCN, UMTS and Bluetooth frequencies.

Antenna configuration and design: The antenna designed at 2.2GHz as centre frequency, consists of a printed slot on a $2\lambda_0 \times 1.5\lambda_0$ ($L \times W$) ground plane fed by a 50Ω microstrip transmission line loaded with an open circuited radial stub. The antenna was fabricated on a double-sided etched Taconic material of ε_r = 2.5 and height (h) 1.57mm. Considering the known broadband advan-